Dalton Transactions

Mechanistic Insight into Oxygen Atom Transfer Reactions by Mononuclear Manganese(IV)-oxo Adducts

Journal:	*Dalton Transactions*
Manuscript ID	DT-ART-12-2020-004436.R1
Article Type:	Paper
Date Submitted by the Author:	12-Feb-2021
Complete List of Authors:	Singh, Priya; University of Kansas College of Liberal Arts and Sciences, Chemistry Stewart-Jones, Eleanor; University of Kansas College of Liberal Arts and Sciences, Chemistry Denler, Melissa; University of Kansas College of Liberal Arts and Sciences, Chemistry Jackson, Timothy; University of Kansas College of Liberal Arts and Sciences, Chemistry

Mechanistic Insight into Oxygen Atom Transfer Reactions by Mononuclear Manganese(IV)-oxo Adducts

Priya Singh,[a] Eleanor Stewart-Jones,[a] Melissa C. Denler,[a] and Timothy A. Jackson*[a]

[a] *The University of Kansas, Department of Chemistry and Center for Environmentally Beneficial Catalysis, 1567 Irving Hill Road, Lawrence, KS 66045, USA.*

*To whom correspondence should be addressed:
Timothy A. Jackson
Phone: (785) 864-3968
taj@ku.edu

Abstract

High-valent metal-oxo intermediates are well known to facilitate oxygen-atom transfer (OAT) reactions both in biological and synthetic systems. These reactions can occur by a single-step OAT mechanism or by a stepwise process initiated by rate-limiting electron transfer between the substrate and the metal-oxo unit. Several recent reports have demonstrated that changes in the metal reduction potential, caused by the addition of Brønsted or Lewis acids, cause a change in sulfoxidation mechanism of Mn^{IV}-oxo complexes from single-step OAT to the multistep process. In this work, we sought to determine if ca. 4000-fold rate variations observed for sulfoxidation reactions by a series of Mn^{IV}-oxo complexes supported by neutral, pentadentate ligands could arise from a change in sulfoxidation mechanism. We examined the basis for this rate variation by performing variable-temperature kinetic studies to determine activation parameters for the reactions of the Mn^{IV}-oxo complexes with thioanisole. These data reveal activation barriers predominantly controlled by activation enthalpy, with unexpectedly small contributions from the activation entropy. We also compared the reactivity of these Mn^{IV}-oxo complexes by a Hammett analysis using *para*-substituted thioanisole derivatives. Similar Hammett ρ values from this analysis suggest a common sulfoxidation mechanism for these complexes. Because the rates of oxidation of the *para*-substituted thioanisole derivatives by the Mn^{IV}-oxo adducts are much faster than that expected from the Marcus theory of outer-sphere electron-transfer, we conclude that these reactions proceed by a single-step OAT mechanism. Thus, large variations in sulfoxidation by this series of Mn^{IV}-oxo centers occurs without a change in reaction mechanism.

Introduction

Atom-transfer reactions involving hydrogen, oxygen, and nitrogen serve as common elementary steps in the functionalization of alkanes and olefins.[1] Because of the difficulty of C—H bond transformations in synthetic settings, the development of new methods to facilitate atom transfer reactions has remained a long-standing challenge. Although synthetically difficult, these reactions are frequently performed in nature by metalloenzymes.[2] Enzymatic systems that perform complex, multistep atom-transfer reactions include the oxygen evolving complex in photosystem II, cytochrome P450 enzymes, and engineered variants of cytochrome $P450_{BM3}$. These enzymes respectively split water into molecular oxygen, protons and electrons; hydroxylate strong C—H bonds and epoxidize olefins; and perform C—H bond amination. Although these enzymes are structurally and functionally diverse, high-valent transition metal species are proposed as common intermediates in such reactions. Therefore, a particular focus has been given to understand the role of high-valent metal-oxo intermediates in both enzymatic and bio-inspired atom-transfer reactions.[2d, 3] Because of the prevalence of both heme and nonheme iron enzymes, the oxygen-atom transfer (OAT) reactions of Fe^{IV}-oxo adducts have been studied in detail.[4] Comparatively less is known concerning the corresponding atom-transfer reactions of Mn^{IV}-oxo complexes, even though such reactions are of potential importance for synthetic catalysts.[5]

The importance of OAT reactions, especially olefin epoxidation, by Mn^{IV}-oxo and Mn^{V}-oxo adducts has also been a long-standing topic of interest.[3c, 5a, 6] Early studies of Mn^{IV}-oxo complexes supported by porphyrin and non-porphyrin ligands showed moderate oxidative reactivity, especially when compared to Fe^{IV}-oxo analogues.[7, 8] More recently, Mn^{IV}-oxo adducts supported by neutral, aminopyridyl ligands have been reported to have reactivities that rival their Fe^{IV}-oxo analogues.[6c] Two of the first members of this class were the $[Mn^{IV}(O)(N4py)]^{2+}$ and $[Mn^{IV}(O)(Bn\text{-}TPEN)]^{2+}$ complexes (Scheme 1). These complexes can

attack strong C—H bonds by a hydrogen-atom transfer mechanism, and perform fairly rapid sulfoxidation of thioanisole and its derivatives.[6c, 6f]

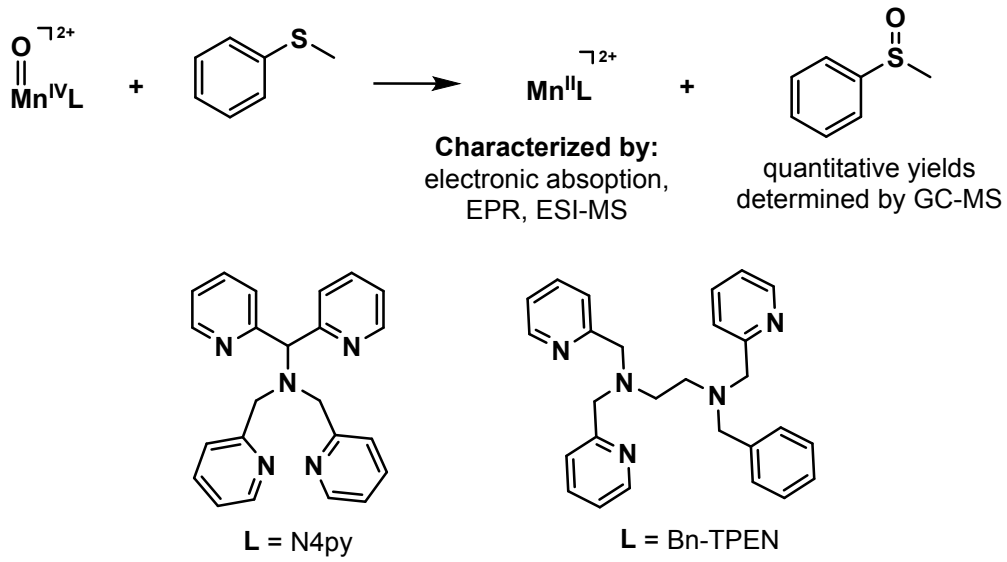

Scheme 1. Sulfoxidation of thioanisole with Mn^{IV}-oxo complexes

Because of their unusually high reactivity in comparison to other Mn^{IV}-oxo adducts, the mechanisms of thioanisole sulfoxidation by $[Mn^{IV}(O)(N4py)]^{2+}$ and $[Mn^{IV}(O)(Bn\text{-}TPEN)]^{2+}$ have been interrogated by both kinetic and computational methods.[6c, 9] These Mn^{IV}-oxo adducts react with excess thioanisole in 2,2,2-trifluoroethanol (TFE) to yield Mn^{II} products and methyl phenyl sulfoxide.[6c, 9] These results support a two-electron oxidation process for thioanisole by these high-valent Mn^{IV}-oxo centers (Scheme 1). Further mechanistic understanding of the oxidation reactions for both $[Mn^{IV}(O)(Bn\text{-}TPEN)]^{2+}$ and $[Mn^{IV}(O)(N4py)]^{2+}$ was achieved by conducting a Hammett analysis with *para*-substituted thioanisole derivatives. These analyses yielded ρ values of -4.4 and -4.6 for $[Mn^{IV}(O)(Bn\text{-}TPEN)]^{2+}$ and $[Mn^{IV}(O)(N4py)]^{2+}$, respectively, at 273 K.[6c, 9] The negative sign of the ρ values is consistent with the electrophilic nature of the Mn^{IV}-oxo adducts, where the fastest rates were observed for thioanisole derivatives with electron-donating substituents.[6c, 9]

Additional investigations of $[Mn^{IV}(O)(N4py)]^{2+}$ and $[Mn^{IV}(O)(Bn\text{-}TPEN)]^{2+}$ showed remarkable rate enhancements for thioanisole oxidation in the presence of Lewis and Brønsted acids. The presence of 6.0 equiv. $Sc^{3+}(OTf)_3$ caused a ca. 2200-fold rate increase for $[Mn^{IV}(O)(N4Py)]^{2+}$,[9] and the addition of 60 equiv. triflic acid caused a ca. 10^5-fold rate enhancement.[10] These large changes in rate were apparently caused by large shifts in the $Mn^{IV/III}$ reduction potentials to more positive values upon the addition of these acids. Reduction potentials for $[Mn^{IV}(O)(N4py)]^{2+}$ and $[Mn^{IV}(O)(Bn\text{-}TPEN)]^{2+}$ shift from 0.80 V and 0.78 V to 1.42 V and 1.36 V, respectively, upon the addition of excess $Sc^{3+}(OTf)_3$.[9] Nam *et al.* postulated that the large OAT rate enhancement of these Mn^{IV}-oxo centers in the presence of acids is due to a change in sulfoxidation mechanism from a single-step OAT pathway to a two-step pathway, with an initial, rate-determining electron-transfer step (Figure 1).[6c, 9-10] A similar switch in mechanism for sulfoxidation of thioanisoles from OAT to rate-limiting electron transfer was observed with $[Fe^{IV}(O)(N4py)]^{2+}$ in presence of Bronsted acid.[11] Here this mechanistic switch also led to a substantial rate enhancement.

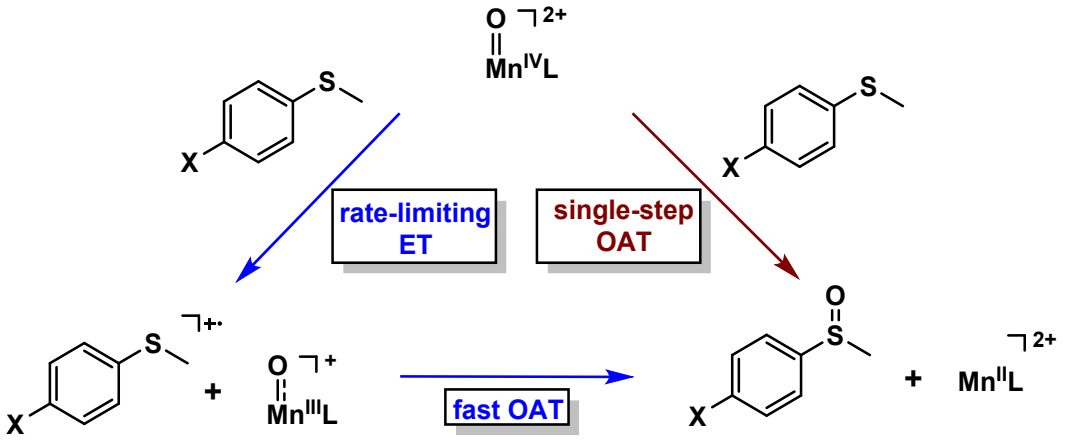

Figure 1. Potential pathways for sulfoxidation of thioanisole derivatives by Mn^{IV}-oxo complexes.

To understand the influence of the local coordination sphere on the OAT reactions of Mn^{IV}-oxo species, our group introduced equatorial ligand perturbations to the N4py scaffold by substituting two of the pyridyl groups with quinolinyl (N2py2Q), benzimidazolyl (N2py2B),

or 3,4-dimethyl-5-methoxypyridyl (^{DMM}N4py) moieties (Figure 2).[12] These ligand perturbations directly modulate the equatorial ligand-field strength. A weakening of the equatorial field should increase the electrophilicity of the Mn^{IV}-oxo unit, which should cause faster reactivity for OAT reactions. Kinetic studies of thioanisole oxidation by this series of complexes revealed the following order for second-order rate constants: $[Mn^{IV}(O)(N2py2Q)]^{2+}$ (**2**) > $[Mn^{IV}(O)(N4py)]^{2+}$ (**1**) > $[Mn^{IV}(O)(N2py2B]^{2+}$ (**4**) > $[Mn^{IV}(O)(^{DMM}N4py)]^{2+}$ (**3**) (Figure 2).[12a, 12b] Thus, the equatorial ligand field exerts a profound influence on the OAT reaction rates. Importantly, the overall rate enhancement for thioanisole oxidation caused by ligand perturbations (ca. 4000-fold) is larger than the rate enhancement caused by the addition of the Lewis acid $Sc^{3+}(OTf)_3$ to $[Mn^{IV}(O)(N4py)]^{2+}$ (2200-fold).[9] In the latter case, the large rate enhancement was attributed by Nam *et al.* to a change in mechanism. Could the large rate enhancement observed for thioanisole oxidation by $[Mn^{IV}(O)(N2py2Q)]^{2+}$ also be due to a change in mechanism?

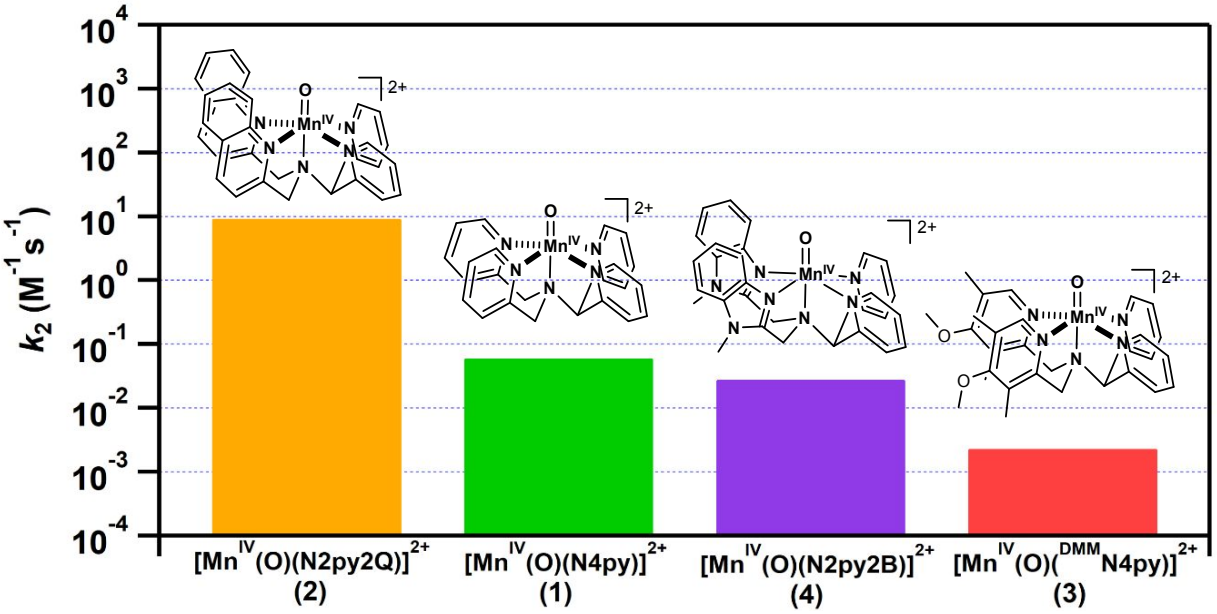

Figure 2. Comparison of thioanisole sulfoxidation rates by Mn^{IV}-oxo species supported by N4py and its derivatives.

In this present work, we performed a detailed kinetic analysis of these reactions to provide a better understanding for the basis for the large OAT rate variations for these Mn^{IV}-oxo

complexes. We used temperature-dependent kinetic experiments to obtain activation parameters for thioanisole oxidation for the four Mn^{IV}-oxo complexes $[Mn^{IV}(O)(N2py2Q)]^{2+}$, $[Mn^{IV}(O)(N4py)]^{2+}$, $[Mn^{IV}(O)(N2py2B)]^{2+}$, and $[Mn^{IV}(O)(^{DMM}N4py)]^{2+}$. These activation parameters are compared to the trend obtained in rate constants for thioanisole oxidation. Additionally, we investigated the electrophilic character of the reactions for this series of complexes through kinetic studies with *para*-substituted thioanisole derivatives. To distinguish between rate-limiting electron-transfer or single-step OAT mechanisms, this collection of rate data were analysed within the framework of Marcus theory for outer-sphere electron transfer. On the basis of this thorough experimental approach, we propose that each of these four Mn^{IV}-oxo complexes reacts with thioanisole and its derivatives by a single-step OAT mechanism.

Experimental Methods

Materials and Instrumentation. All chemicals and solvents were ACS reagent grade and were purchased from commercial vendors. Iodosobenzene (PhIO) was prepared from iodosobenzene diacetate as per a reported procedure.[13] 4-*tert*butylthioanisole was synthesized by reacting 4-*tert*-butylthiophenol with 1.5 equiv. methyl iodide in dry THF and in the presence of 1.1 equiv. NaH. This reaction was stirred for 48 hours at ambient temperature. This mixture was then treated with 10 mL of 5 M NaOH, stirred for 5 min, and then extracted with 15 mL dichloromethane. The organic layer was dried over anhydrous sodium sulfate and the product was isolated as a pale-yellow liquid by removing the solvent (89% yield). The crude product was purified with a silica column using pure hexanes to obtain 4-*tert*-butylthioanisole as a white solid (Figure S1).

Electrochemical experiments to determine oxidation potentials of thioanisole derivatives were performed using cyclic voltammetry with an Epsilon potentiostat. For these experiments,

a glassy carbon working electrode, a platinum auxiliary electrode and a Ag/AgCl quasi-reference electrode were used, with ferrocene/ferrocenium potential as an external reference. These experiments used 2 mM solutions of each thioanisole derivative in 2,2,2-trifluoroethanol (TFE), with 0.1 M *n*-Bu_4NPF_6 as supporting electrolyte at 298 K (Figure S11).

All kinetic experiments were performed by electronic absorption spectroscopy. Electronic absorption data were collected on either an Agilent 8453 or Cary 50 Bio spectrometer. Temperature control was achieved using either a Unisoku (USP-203-A) cryostat or a Quantum Northwest cryostat (t2 Sport).

General Procedure for Formation of Mn^{IV}-oxo Complexes. The series of ligands N4py, N2py2Q, ^{DMM}N4py, and N2py2B, and their corresponding Mn^{II} complexes were synthesized according to previously reported methods.[12a, 12b, 14] Mn^{IV}-oxo adducts were prepared *in situ* by oxidizing the corresponding Mn^{II} complexes with iodosobenzene (PhIO) in TFE at 25 ℃. Maximal formation of $[Mn^{IV}(O)(N4py)]^{2+}$ and $[Mn^{IV}(O)(N2py2B)]^{2+}$ was achieved using 2.5 equiv. PhIO. For the generation of $[Mn^{IV}(O)(^{DMM}N4py)]^{2+}$, 1.2 equiv. PhIO was used to acheive maximal formation, and 10 equiv. PhIO were needed to achieve maximal formation of $[Mn^{IV}(O)(N2py2Q)]^{2+}$, which is the least stable Mn^{IV}-oxo adduct in this series. The formation of Mn^{IV}-oxo adducts was assessed using electronic absorption spectroscopy (Figure S2) and comparing the optical features observed to those previously reported for these complexes.[12a, 12b]

Kinetic Experiments. Rate constants were determined under pseudo-first-order conditions, where a Mn^{IV}-oxo complex was formed *in situ* and then treated with an excess of thioanisole or its derivatives. A representative procedure for $[Mn^{IV}(O)(N4py)]^{2+}$ is as follows. The intermediate $[Mn^{IV}(O)(N4py)]^{+2}$ was prepared *in situ* by oxidizing a 1 mM $[Mn^{II}(OTf)(N4py)](OTf)$ (0.002 mmol) solution with PhIO (0.005 mmol) in 2.0 mL TFE at 25

°C. The appearance of an electronic absorption band at 950 nm indicated the formation of the Mn^{IV}-oxo adduct. Once the formation was completed, a 0.1 mL aliquot of a solution containing an excess of *para*-X-thioanisole (X = OMe, ^{t}Bu, H, F, Br, and CN) in TFE was added to the solution of the Mn^{IV}-oxo adduct in the cuvette, giving a final volume of 2.1 mL. The decay of the absorption band at 950 nm was monitored, and the resulting time trace was fit to a pseudo-first order kinetic model to give an observed rate (k_{obs})(Figure S3). Solubility issues with higher concentrations of *p*-Br-thioanisole, *p*-CN-thioanisole and *p*-F-thioanisole in TFE were overcome by dissolving these substrates in CH_2Cl_2. The same procedure was adopted for other Mn^{IV}-oxo intermediates derived from the $[Mn^{II}(OH)_2(N2py2Q)](OTf)_2$, $[Mn^{II}(OTf)(^{DMM}N4py)](OTf)$, and $[Mn^{II}(OH)_2(N2py2B)](OTf)$ complexes. Each experiment was performed in triplicate with varied equivalents of *para*-X-thioanisole. Plots of the pseudo-first-order rate constants versus substrate concentration were fit to a linear equation to determine the second-order rate constants (k_2) for these reactions (see SI, figure S6-S8).

Determination of Activation Parameters. Each Mn^{IV}-oxo complex was treated with an excess of thioanisole at four different temperatures spaced apart by 10^{o} C to obtain activation parameters for these reactions. In each reaction, a 0.1 mL aliquot of thioanisole (40 equiv.) was added to the Mn^{IV}-oxo adduct and the decay of the corresponding Mn^{IV}-oxo feature in the near-IR region was fit to a pseudo-first-order model to obtain k_{obs}. Each experiment was performed in triplicate at temperatures suitable for accurate measurements of the given reaction. The appropriate temperature range varied depending on the OAT reactivity of each Mn^{IV}-oxo complex. Eyring plots for these reactions were obtained by plotting $\ln(k_{obs}/T)$ versus 1/T (in Kelvin), and activation parameters $\Delta H^{‡}$ and $\Delta S^{‡}$ were determined from a linear fit to the data using the Eyring equation,

$$\ln\frac{k}{T} = \frac{-\Delta H^{‡}1}{R\ T} + \ln\frac{k_B}{h} + \frac{\Delta S^{‡}}{R} \qquad (1)$$

Where k represents the pseudo-first order rate constant (k_{obs}) obtained for the thioanisole oxidation by **1 - 4** at variable temperature range depending on the identity of the complex. $\Delta H^{\ddagger}$ and $\Delta S^{\ddagger}$ are the enthalpy and entropy of activation needed to access the transition state from the free reactants, while k_B, h and R are constants with values of 1.38×10^{-23} J·K^{-1}, 6.626×10^{-34} J·s and 8.315 J·mol^{-1}·K^{-1}, respectively.

Results and Discussion

Activation Parameters. To better understand the large rate variations for the set of Mn^{IV}-oxo complexes (**1 – 4**), we determined activation parameters for thioanisole oxidation. For this analysis, we monitored the decay of the characteristic near-IR absorption band of the Mn^{IV}-oxo adducts (centered around 940 nm) upon the addition of 40 equiv. thioanisole and fit this decay to obtain a pseudo-first order rate constant (k_{obs}) (Figure S3). For each complex, the decay followed pseudo-first-order behavior to at least 3 half-lives, validating our approach. These experiments were repeated at various fixed temperatures, with the precise temperature range depending on the Mn^{IV}-oxo complex. For each Mn^{IV}-oxo complex, a plot of ln(k_{obs}/T) versus 1/T showed a linear correlation and could be fit using the Eyring equation (Figure 3). This analysis gave the activation enthalpies ($\Delta H^{\ddagger}$) and entropies ($\Delta S^{\ddagger}$) in Table 1. The free energies of activation ($\Delta G^{\ddagger}$) at 298 K are also given in Table 1. From these data, it is clear that the previously reported k_2 values for the sulfoxidation of thioanisole by the series of Mn^{IV}-oxo complexes trend with the experimentally determined $\Delta G^{\ddagger}$ values. For example, **2** shows the largest k_2 value and the smallest $\Delta G^{\ddagger}$ of 17.7 kcal/mol, while **3** has the smallest k_2 value and largest $\Delta G^{\ddagger}$ of 23.0 kcal/mol. Thus, among this set of structurally similar complexes, there are variations in the free energy barrier for sulfoxidation of over 5 kcal/mol. These variations in the values of $\Delta G^{\ddagger}$ are predominantly governed by changes in $\Delta H^{\ddagger}$, signifying that enthalpic

contributions govern the rates of these reactions. In particular, the reaction of **2** with thioanisole has the smallest $\Delta H^{\ddagger}$ of 14.7 kcal/mol, while the more sluggish oxidants **3** and **4** show $\Delta H^{\ddagger}$ for thioanisole sulfoxidation near 21 kcal/mol. The entropic contribution to the free energy of activation ($T\Delta S^{\ddagger}$), although expected to be negative, was unusually small for a bimolecular reaction (Table 1).

Table 1. Activation parameters (kcal/mol) and second-order rate constants ($M^{-1}s^{-1}$) for sulfoxidation reactions of Mn^{IV}-oxo complexes (1mM solution in TFE) with various substrates at 298 K.

Complex	substrate	$\Delta H^{\ddagger}$	$T\Delta S^{\ddagger}$	$\Delta G^{\ddagger}$	k_2
$[Mn^{IV}(O)(N4py)]^{2+}$ (**1**)	thioanisole	19.9	-1.10	21.0	1.2×10^{-1}
$[Mn^{IV}(O)(N2py2Q)]^{2+}$ (**2**)	thioanisole	14.7	-3.00	17.7	9.2
$[Mn^{IV}(O)(^{DMM}N4py)]^{2+}$ (**3**)	thioanisole	21.2	-1.80	23.0	2.3×10^{-3}
$[Mn^{IV}(O)(N2py2B)]^{2+}$ (**4**)	thioanisole	20.7	-0.90	21.6	2.8×10^{-2}
$[Mn^{IV}(O)(N4py)]^{2+}$ + 60 equiv. HOTf [a]	*p*-CN-thioanisole	15.1	-0.40	15.5	2.5
$[Mn^{V}(O)(TDCPP)]^{+}$ [b]	*p*-NH_2-thioanisole	7.0	-13.1	20.1	2.6×10^{-2}
$[Mn^{V}(O)(TBP_8Cz)]$ [c]	dibutyl sulfide	16.0	-6.00	22.0	3.8×10^{-4}

[a] Data from reference 10. [b] Data from reference 18. [c] Data from reference 19.

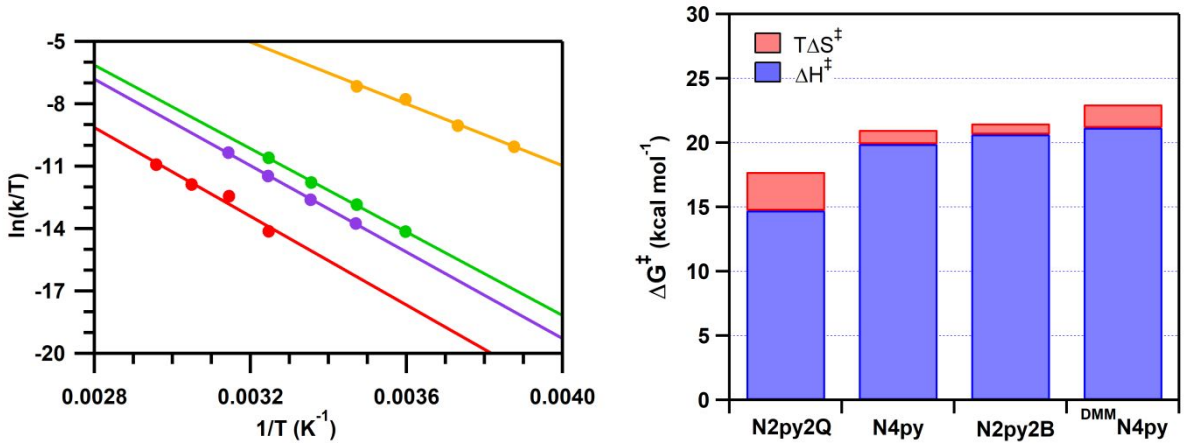

Figure 3. Eyring plot of ln(k/T) versus 1/T for the reaction of Mn^{IV}-oxo complexes with thioanisole (left) and comparison of activation parameters determined from this Eyring analysis of variable-temperature kinetic data (right). In the right-hand plot, the blue bars represent the activation enthalpies, $\Delta H^{\ddagger}$ in kcal/mol, and the red bars represent $T\Delta S^{\ddagger}$ in kcal/mol at 298 K.

Nam *et al.* have investigated the sulfoxidation of 4-(methylthio)benzonitrile by **1** in the presence of 60 equiv. HOTf and determined $\Delta H^{\ddagger}$ = 15.1 kcal/mol and $\Delta S^{\ddagger}$ = -1.2 cal/mol·K ($T\Delta S^{\ddagger}$ = -0.4 kcal/mol at 298 K). These parameters are shown in Table 1 for comparison. The small activation entropy was postulated to be the result of an outer-sphere electron-transfer

mechanism, rather than a single-step OAT mechanism.[15] Further support for an outer-sphere electron-transfer mechanism was provided by the accordance of the rate data with that expected from Marcus theory. On the basis of this precedent, the low activation entropies for thioanisole sulfoxidation by **1** - **4** could imply an outer-sphere electron-transfer mechanism. However, there are alternative explanations for a low activation entropy. For example, the Mn^{IV}-oxo species and thioanisole could form precursor complexes in an initial equilibrium step, and then traverse the transition-state barrier. The formation of precursor complexes has been observed in hydrocarbon oxidation by Mn^{IV}-oxo species.[16] We attempted to evaluate this prediction by measuring k_{obs} values for thioanisole oxidation by **2** at higher thioansiole concentrations. The formation of a pre-equilibrium between the free reactants and a precursor complex should be manifested in saturation of k_{obs} at high thioanisole concentrations.[16-17] Unfortunately, we were unable to test this prediction, as the limited solubility of the substrate prevented us from collecting reliable kinetic data at substrate concentrations beyond 70.0 mM (70 equiv. relative to the Mn^{IV}-oxo complex).

Further evidence against concluding an electron-transfer mechanism for thioanisole oxidation by Mn^{IV}-oxo on the basis of the small activation entropies comes from a previous study of thioanisole oxidation by **1**.[10] From that work, it was shown that the rate of thioanisole sulfoxidation does not follow that expected from Marcus theory of outer-sphere electron transfer, and an OAT mechanism was proposed.[10] Therefore, we conclude that the entropic contributions to the activation energies of **1** – **4** cannot be used to infer the mechanism for thioanisole oxidation by these Mn^{IV}-oxo compounds.

Since some of these Mn^{IV}-oxo complexes show such rapid reactions towards thioanisole, it is warranted to compare these results with activation parameters for Mn^{V}-oxo species. There are only few examples of experimental activation parameters for sulfoxidation by Mn^{V}-oxo complexes, and these show a range of values for activation parameters. For example,

sulfoxidation of 4-(methylthio)aniline by $[Mn^{V}(O)(TDCPP)]^{+}$ (TDCPP = 5,10,15,20-tetrakis(2,6-dichlorophenyl)porphyrin)[18] and sulfoxidation of dibutyl sulfide by $[Mn^{V}(O)(TBP_{8}Cz)]$ (TBP8Cz = octakis(*p*-tert-butylphenyl)corrolazinato^{3-})[19] revealed large negative entropic contributions ($T\Delta S^{\ddagger}$) of -13.1 and -6.0 kcal/mol at 298 K, respectively, with activation enthalpies of 7 and 16 kcal/mol, respectively. Intriguingly, while the sulfoxidation reactions of these Mn^{V}-oxo adducts show substantially smaller activation enthalpies compared to the reactions of the Mn^{IV}-oxo complexes **1** – **4**, the larger activation entropies for the former reactions result in free energy barriers on par with those of the Mn^{IV}-oxo sulfoxidation reactions. These data are summarized in Table 1.

OAT reactivity of thioanisole derivatives with Mn^{IV}-Oxo adducts 1 - 4. To further probe the mechanism of sulfoxidation by complexes **1** - **4**, kinetic studies were performed with thioanisole derivatives substituted at the *para* position with a range of electron-rich and electron-deficient substituents (Table 2). For this analysis, we included reactions for which the treatment of the Mn^{IV}-oxo complex with an excess of a *para*-X-thioanisole showed a pseudo-first-order decay of the Mn^{IV}-oxo optical feature in the near-IR region. These experiments were repeated by varying the concentrations of thioanisole substrates. Oxidation reactions of many thioanisole derivatives with **4** did not result in clean kinetics (*i.e.*, the decay rate of the Mn^{IV}-oxo absorption feature could not be fit to pseudo-first order model). As a result, second order rate constant could not be determined for thioanisole derivatives except for thioanisole and *p*-^{t}Bu-thioanisole. Additional information describing our attempts at probing the reactivity of **4** with *para*-X-thioanisole derivatives is provided in the Supporting Information.

Table 2. Hammett parameters and second-order rate constants (k_2) determined in reaction of **1**, **2** and **3** with *p*-substituted thioanisole derivatives in CF_3CH_2OH at 298 K.

			k_2 (M^{-1} s^{-1})			k_X/k_H			$log(k_X/k_H)$		
Substrate	σ_p[b]	σ_p^+[b]	**1**	**2**	**3**	**1**	**2**	**3**	**1**	**2**	**3**
p-MeO-thioanisole	-0.27	-0.78	1.00×10^{1}		1.10×10^{1}	83.6		4.74×10^{3}	1.92		3.67
p-^{t}Bu-thioanisole	-0.20	-0.26	4.58×10^{-1}		1.24×10^{-1}	3.82		5.36×10^{1}	0.58		1.73
thioanisole	0	0	1.20×10^{-1}	9.20	2.31×10^{-3}	1.00	1.00	1.00	0.00	0.00	0.00
p-F-thioanisole	0.062	0.07	3.89×10^{-2}	5.40	1.69×10^{-3}	0.32	0.59	0.73	-0.49	-0.23	-0.14
p-Br-thioanisole	0.23	0.15	1.50×10^{-2}	2.21	1.03×10^{-3}	0.13	0.24	0.45	-0.90	-0.62	-0.35
p-CN-thioanisole	0.66	0.66		1.55×10^{-2}			0.002			-2.79	

[a] Hammett constants have been taken from the literature.[20] [b] Relative rate constants (k/k_0) have been obtained by dividing k_2 for reactions with *para*-thioanisoles by k_2 for reactions with thioanisole.

For the Mn^{IV}-oxo adducts **1** - **3**, a linear correlation between k_{obs} and substrate concentration was obtained for several *para*-X-thioanisole substrates, giving second-order rate constants (k_2). Using these k_2 values, a Hammett plot of $\log(k_x/k_H)$ against σ^+ was constructed. We chose to employ the σ^+ values for this correlation rather than σ, as we obtained a better fit with the former. Each plot shows a linear correlation with a negative slope (ρ; see Figure 4). The negative sign of the slopes are in consonance with the electrophilic nature of the Mn^{IV}-oxo adducts. The similarity in ρ values, which span the narrow range of -2.9 to -4.4, also suggest that these complexes follow the same sulfoxidation mechanism for this set of substrates.

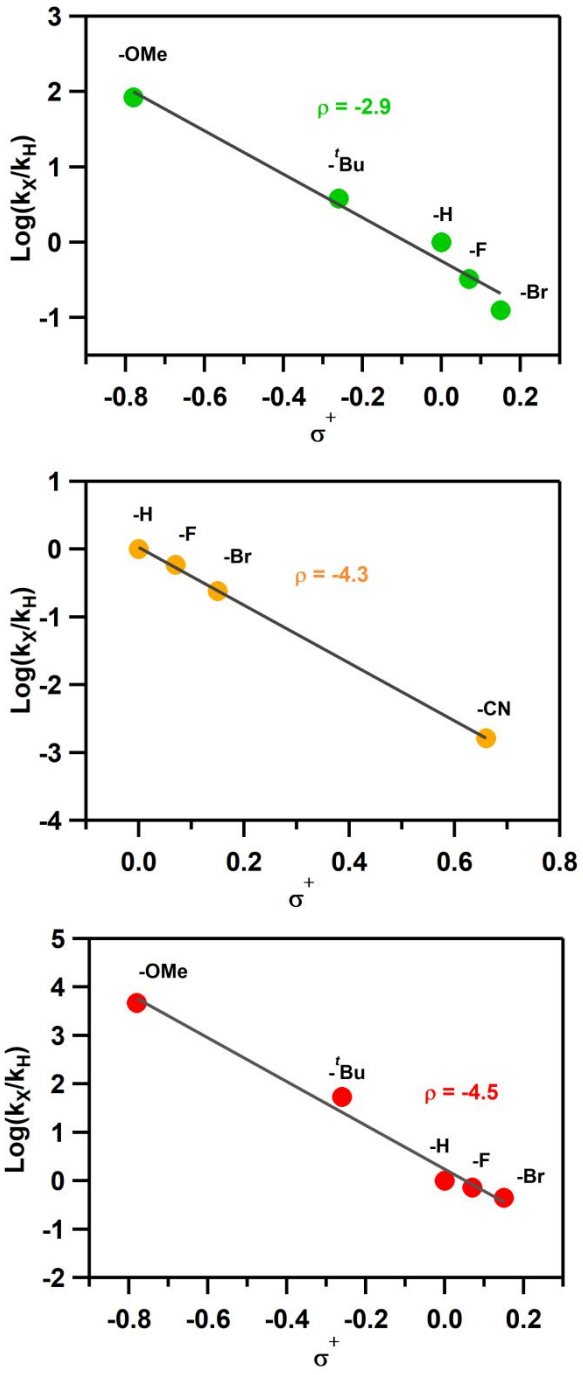

Figure 4. Hammett plots of $\log(k_X/k_H)$ against σ+ of para-X-thioanisole derivatives by **1** (green), **2** (orange) and **3** (red) at 298 K.

Nam *et al.* have previously performed a Hammett analysis of sulfoxidation by **1** using *para*-X-thioanisole derivatives at 273 K.[9] Using a σ value to describe the effects of the substituents, they determined ρ = -4.6. For a direct comparison, we replotted their data using the σ^+ values that we have used in this present analysis (Figure S4). The use of the σ^+ values for the

previously reported rates gives a slope (ρ) of -2.4, which is very similar to the value of -2.9 at 298 K (Figure 4).

We also plotted the log of our second-order rate constants for *para*-X-thioanisole oxidation versus the oxidation potentials of the substrates. From this analysis, we see that the rates of the reactions of **1** and **2** are linearly correlated with the substrate oxidation potential, with large negative slopes of -8.9 to -6.6 V^{-1} (Figure S5). The reactions of complex **3** follow the general trend of increasing reaction rate with decreasing substrate oxidation potential, but this trend is not as linear as that observed for complexes **1** and **2** (Figure S5). In some previous studies, the slopes of log(k_2) values for metal-based sulfoxidation reactions versus substrate oxidation potential have been used to distinguish single-step OAT versus rate-limiting electron-transfer mechanisms, with larger slopes of -7 to -10 V^{-1} marking the latter mechanism.[21] However, there does not seem to be a consensus in this approach. In other cases, larger slopes of -6 to -8 V^{-1} were observed for reactions attributed to a single-step OAT mechanism.[10-11, 22] Thus, although the steep slope observed for sulfoxidation by **3** is unusual, its mechanistic relevance is unclear.

To further probe the nature of the rate-determining step in thioanisole sulfoxidation by the Mn^{IV}-oxo adducts **1 - 3**, we compared the experimental rate constants for the oxidation of *para*-X-thioanisole derivatives with that predicted from the driving force for an outer-sphere electron-transfer reaction. This approach has been previously employed by Fukuzumi, Nam, and co-workers to determine if substrate oxidation reactions by a metal-based oxidant proceed by a rate-limiting atom-transfer step or by an outer-sphere electron-transfer step.[10] Following this approach, we employ eqn. 2, which relates the outer-sphere electron-transfer rate constant (k_{et}) to the reaction driving force ΔG_{et} according to the Marcus theory of adiabatic outer-sphere electron transfer.

$$k_{et} = Z \exp[-(\lambda/4)(1+ \Delta G_{et}/\lambda)^2/k_B T] \qquad (2)$$

In this equation, Z is the collision frequency, which we have assigned a value of 1×10^{11} $M^{-1}s^{-1}$ at 25 °C; λ is the reorganization energy of electron transfer in eV; ΔG_{et} is the driving force in eV and is defined as $\Delta G_{et} = -e(E_{red}-E_{ox})$); and k_B and T are the Boltzmann constant and absolute temperature, respectively. To demonstrate the use of this approach, Figure 5 shows rate constants for reactions of one-electron reductants and **1** at 273 K (black dots), reported by Nam, Fukuzumi, and co-workers.[10] These points can be well-fit using eqn. 1 and the known values for E_{red} and E_{ox} for **1** and the substrates, respectively. The only fitted parameter in this procedure is the reorganization energy (λ = 2.22 eV), which yields a value reasonable for outer-sphere electron transfer with a transition metal complex.[10] For further comparison, Figure 5 also demonstrates how the rate constants for sulfoxidation of thioanisole derivatives by **1** in the presence of trific acid (blue dots), which were reported by Nam, Fukuzumi, and co-workers, are also well-fit by eqn. 1.[10] The reorganization energies from these fits are similar to those obtained by Nam and co-workers from a previous analysis.[9-10] The ability to fit these rate constants by this method provides support for an outer-sphere electron transfer mechanism for this reaction, as demonstrated previously.[10-11]

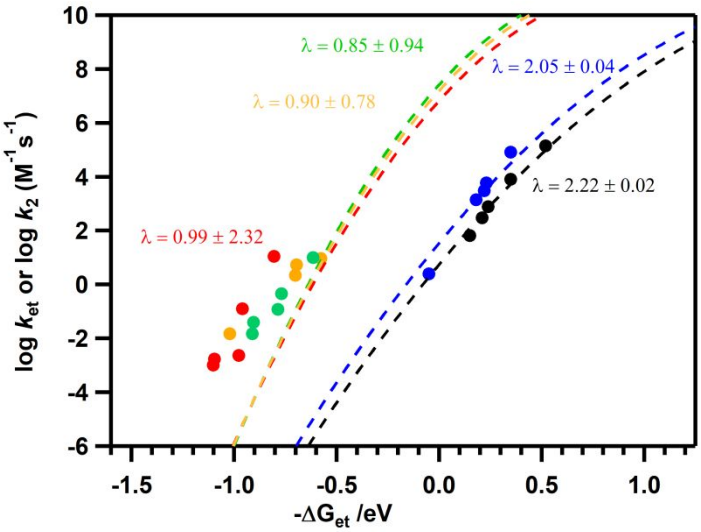

Figure 5. Plot of log k_2 for sulfoxidation of para thioanisole derivatives vs driving force of electron transfer [$-\Delta G_{et}$= $e(E_{red}-E_{ox})$] from thioanisoles to $[Mn^{IV}(O)N4py]^{2+}$ (green dots), $[Mn^{IV}(O)2pyN2Q]^{2+}$ (orange dots), and $[Mn^{IV}(O)^{DMM}N4py]^{2+}$ (red dots) at 298 K, and $[Mn^{IV}(O)N4py]^{2+}$ in presence of HOTf (blue dots)[10] at 273 K. Black dots represents the driving force dependence of the rate constants (log k_{et}) of the ET from one-electron reductants to

$[Mn^{IV}(O)N4py]^{2+}$ at 273 K.[10] The larger errors associated with the reorganization energies reflect the poor fits to the experimental data.

Nam *et al.* have previously applied this type of analysis for the sulfoxidation reactions of thioanisoles by **1** at 273 K.[10] Because the reaction rates were faster than those that predicted for outer-sphere electron by Marcus theory, it was concluded that electron-transfer cannot be the rate-limiting step.[10] In order to explore the mechanistic pathways involved in sulfoxidation by **2** and **3**, we extend this analysis to these complexes. We also examined our data collected for **1** at 298 K, as a change in temperature could result in a change in reaction mechanism.[23] We attempted to fit the rate constants obtained from sulfoxidation reactions of *p*-thioanisoles by the Mn-oxo adducts **1 - 3** at 298 K using the Marcus theory model. In this approach, we calculated the $-\Delta G_{et}$ terms using the previously reported reduction potentials of **1 - 3**[12b] and the oxidation potentials of *p*-X-thioanisole obtained at 298 K.[24] These data are collected in Table 3. In our fits, the reorganization energy (λ) was floated to best fit the data. As shown in Figure 5, we are unable to adequately fit the experimental data points (red, green and yellow spheres in Figure 5) to the behaviour predicted by Marcus theory (red, yellow, and green dashed traces in Figure 5). In all cases, the predicted $\log(k_{et})$ versus $-\Delta G_{et}$ curves yield reaction rates far slower than those observed experimentally. Thus, the experimental reactions rates are much faster than expected for an outer-sphere electron-transfer reaction at these driving forces. On this basis, we conclude that the reactions of **1-3** with the *para*-substituted thioanisole substrates all proceed by a single-step OAT mechanism that avoids higher barriers associated with an outer-sphere electron-transfer mechanism.

Table 3. Second order rate constants of sulfoxidation reactions of thioanisole derivatives by **1**, **2** and **3** with driving force of electron transfer ($-\Delta G_{et}$) and one-electron oxidation potentials (E_{ox}) of *p*-X-thioanisoles at 298 K.

		k_2 (M^{-1} s^{-1})			ΔG_{et}[b] (eV)		
Substrate	E_{ox}[a]	**1**	**2**	**3**	**1**	**2**	**3**
p-MeO-thioanisole	1.42	1.00×10^{1}	-	1.10×10^{1}	-0.62	-	-0.81
p-^{t}Bu-thioanisole	1.57	4.58×10^{-1}	-	1.24×10^{-1}	-0.77	-	-0.96
thioanisole	1.59	1.20×10^{-1}	9.2	2.31×10^{-3}	-0.79	-0.58	-0.98
p-F-thioanisole	1.70	3.89×10^{-2}	5.4	1.69×10^{-3}	-0.90	-0.69	-1.09
p-Br-thioanisole	1.71	1.50×10^{-2}	2.21	1.03×10^{-3}	-0.91	-0.70	-1.10
p-CN-thioanisole	2.03	-	1.55×10^{-2}	-	-	-1.02	-

[a]oxidation potentials (E_{pc}) of *p*-X-thioanisoles were obtained by cyclic voltammetry in CF_3CH_2OH containing 0.10 M *n*-Bu_4NPF_6 as supporting electrolyte. [b] $-\Delta G_{et}$ was determined by $[-\Delta G_{et} = e(E_{red}-E_{ox})]$, where one-electron reduction potential of **1** (0.80 V vs SCE), **2** (1.01 V vs SCE) and **3** (0.61 V vs SCE) were used.

Conclusions.

In this work, we have presented a comparative study of sulfoxidation reactions of Mn^{IV}-oxo complexes supported by neutral pentadentate N5 ligands with different donor properties. Previous work had established that modulations in the equatorial ligand field of these complexes caused a dramatic effect on sulfoxidation reactivity, with a ca. 4000-fold rate enhancement.[12a] The basis for this variation in rates was investigated here by applying an Eyring analysis to variable-temperature kinetic data, where activation parameters for thioanisole sulfoxidation were determined. This analysis revealed that the reaction barriers are controlled by the enthalpy of activation, with unexpectedly small entropic contributions. While small entropies of activation have previously been taken as evidence for a rate-limiting outer-sphere electron-transfer step,[10, 15] they could simply be an outcome of the formation of a precursor complex. We also explored the reactivity of these Mn^{IV}-oxo complexes with various derivatives of thioanisole. While reactions of **4** with thioanisole derivatives were challenging, linear Hammett plots were obtained for rest of the complexes in the series. The similar slopes obtained in Hammett analyses of sulfoxidation by **1** - **3** ruled out a possible switch in mechanism from single-step OAT to rate-limiting electron transfer. This conclusion was further supported by attempts to fit the reaction rates with the Marcus theory of outer-sphere electron transfer. In this case, we observed that the reaction rates are far more rapid than that

expected on the basis of the driving force for electron transfer. This observation is a hallmark of a concerted mechanism that avoids higher barriers associated with a stepwise process. Thus, remarkable rate enhancements for OAT reactions can be achieved for Mn^{IV}-oxo complexes without a change in reaction mechanism.

Conflicts of Interest.

There are no conflicts to declare.

Acknowledgements.

This work was supported by the U.S. D.O.E. (DE-SC0016359). M. C. D. was supported by the NIH Graduate Traineeship T32 GM08545. Support for the NMR instrumentation was provided by NIH Shared Instrumentation Grant # S10OD016360.

References.

1. a) L. Capaldo and D. Ravelli, *European Journal of Organic Chemistry*, 2017, **2017**, 2056-2071; b) T. Kojima, R. A. Leising, S. Yan and L. Que, *Journal of the American Chemical Society*, 1993, **115**, 11328-11335; c) Y. Liu, T. You, T.-T. Wang and C.-M. Che, *Tetrahedron*, 2019, **75**, 130607; d) F. Marchetti, C. Pettinari, C. Di Nicola, A. Tombesi and R. Pettinari, *Coordination Chemistry Reviews*, 2019, **401**, 213069; e) L. M. Stateman, K. M. Nakafuku and D. A. Nagib, *Synthesis (Stuttg)*, 2018, **50**, 1569-1586; f) X. Tang, X. Jia and Z. Huang, *Chemical Science*, 2018, **9**, 288-299.
2. a) H. S. Fernandes, C. S. S. Teixeira, S. F. Sousa and N. M. F. S. A. Cerqueira, *Molecules*, 2019, **24**, 2462; b) R. H. Holm, *Chemical Reviews*, 1987, **87**, 1401-1449; c) F. Schwizer, Y. Okamoto, T. Heinisch, Y. Gu, M. M. Pellizzoni, V. Lebrun, R. Reuter, V. Köhler, J. C. Lewis and T. R. Ward, *Chemical Reviews*, 2018, **118**, 142-231; d) T. K. Hyster, C. C. Farwell, A. R. Buller, J. A. McIntosh and F. H. Arnold, *Journal of the American Chemical Society*, 2014, **136**, 15505-15508.
3. a) A. S. Borovik, *Chemical Society Reviews*, 2011, **40**, 1870-1874; b) T. Taguchi, R. Gupta, B. Lassalle-Kaiser, D. W. Boyce, V. K. Yachandra, W. B. Tolman, J. Yano, M. P. Hendrich and A. S. Borovik, *Journal of the American Chemical Society*, 2012, **134**, 1996-1999; c) M. Guo, T. Corona, K. Ray and W. Nam, *ACS Central Science*, 2019, **5**, 13-28.
4. a) M. Srnec, S. D. Wong, J. England, L. Que, Jr. and E. I. Solomon, *Proc Natl Acad Sci U S A*, 2012, **109**, 14326-14331; b) M. Srnec, S. D. Wong, M. L. Matthews, C. Krebs, J. M. Bollinger and E. I. Solomon, *Journal of the American Chemical Society*, 2016, **138**, 5110-5122; c) M. Srnec, S. D. Wong and E. I. Solomon, *Dalton Transactions*, 2014, **43**, 17567-17577; d) W. Ye, D. M. Ho, S. Friedle, T. D. Palluccio and E. V.

Rybak-Akimova, *Inorg Chem*, 2012, **51**, 5006-5021; e) J. Hohenberger, K. Ray and K. Meyer, *Nature Communications*, 2012, **3**, 720.

5. a) V. A. Larson, B. Battistella, K. Ray, N. Lehnert and W. Nam, *Nature Reviews Chemistry*, 2020, **4**, 404-419; b) S. Fukuzumi, T. Kojima, Y.-M. Lee and W. Nam, *Coordination Chemistry Reviews*, 2017, **333**, 44-56.
6. a) A. A. Massie, A. Sinha, J. D. Parham, E. Nordlander and T. A. Jackson, *Inorg Chem*, 2018, **57**, 8253-8263; b) K. Ray, F. F. Pfaff, B. Wang and W. Nam, *Journal of the American Chemical Society*, 2014, **136**, 13942-13958; c) X. Wu, M. S. Seo, K. M. Davis, Y.-M. Lee, J. Chen, K.-B. Cho, Y. N. Pushkar and W. Nam, *Journal of the American Chemical Society*, 2011, **133**, 20088-20091; d) J. R. Mayfield, E. N. Grotemeyer and T. A. Jackson, *Chemical Communications*, 2020, **56**, 9238-9255; e) H. M. Neu, R. A. Baglia and D. P. Goldberg, *Accounts of Chemical Research*, 2015, **48**, 2754-2764; f) D. F. Leto, R. Ingram, V. W. Day and T. A. Jackson, *Chemical Communications*, 2013, **49**, 5378-5380; g) H. M. Neu, T. Yang, R. A. Baglia, T. H. Yosca, M. T. Green, M. G. Quesne, S. P. de Visser and D. P. Goldberg, *Journal of the American Chemical Society*, 2014, **136**, 13845-13852; h) H. M. Neu, M. G. Quesne, T. Yang, K. A. Prokop-Prigge, K. M. Lancaster, J. Donohoe, S. DeBeer, S. P. de Visser and D. P. Goldberg, *Chemistry – A European Journal*, 2014, **20**, 14584-14588; i) P. Leeladee and D. P. Goldberg, *Inorg Chem*, 2010, **49**, 3083-3085; j) R. A. Baglia, M. Dürr, I. Ivanović-Burmazović and D. P. Goldberg, *Inorg Chem*, 2014, **53**, 5893-5895; k) B. S. Mandimutsira, B. Ramdhanie, R. C. Todd, H. Wang, A. A. Zareba, R. S. Czernuszewicz and D. P. Goldberg, *Journal of the American Chemical Society*, 2002, **124**, 15170-15171.
7. a) T. H. Parsell, R. K. Behan, M. T. Green, M. P. Hendrich and A. S. Borovik, *Journal of the American Chemical Society*, 2006, **128**, 8728-8729; b) T. H. Parsell, M.-Y. Yang and A. S. Borovik, *Journal of the American Chemical Society*, 2009, **131**, 2762-2763; c) S. Shi, Y. Wang, A. Xu, H. Wang, D. Zhu, S. B. Roy, T. A. Jackson, D. H. Busch and G. Yin, *Angewandte Chemie International Edition*, 2011, **50**, 7321-7324; d) D. G. Karmalkar, X.-X. Li, M. S. Seo, M. Sankaralingam, T. Ohta, R. Sarangi, S. Hong and W. Nam, *Chemistry*, 2018, **24**, 17927-17931.
8. a) R. Zhang, J. H. Horner and M. Newcomb, *Journal of the American Chemical Society*, 2005, **127**, 6573-6582; b) M. Schappacher and R. Weiss, *Inorg Chem*, 1987, **26**, 1189-1190; c) J. T. Groves and M. K. Stern, *Journal of the American Chemical Society*, 1988, **110**, 8628-8638; d) R. D. Arasasingham, G. X. He and T. C. Bruice, *Journal of the American Chemical Society*, 1993, **115**, 7985-7991; e) W. Adam, C. Mock-Knoblauch, C. R. Saha-Möller and M. Herderich, *Journal of the American Chemical Society*, 2000, **122**, 9685-9691.
9. J. Chen, Y.-M. Lee, K. M. Davis, X. Wu, M. S. Seo, K.-B. Cho, H. Yoon, Y. J. Park, S. Fukuzumi, Y. N. Pushkar and W. Nam, *Journal of the American Chemical Society*, 2013, **135**, 6388-6391.
10. J. Chen, H. Yoon, Y.-M. Lee, M. S. Seo, R. Sarangi, S. Fukuzumi and W. Nam, *Chemical Science*, 2015, **6**, 3624-3632.
11. J. Park, Y. Morimoto, Y.-M. Lee, W. Nam and S. Fukuzumi, *Journal of the American Chemical Society*, 2011, **133**, 5236-5239.
12. a) M. C. Denler, A. A. Massie, R. Singh, E. Stewart-Jones, A. Sinha, V. W. Day, E. Nordlander and T. A. Jackson, *Dalton Trans*, 2019, **48**, 5007-5021; b) A. A. Massie, M. C. Denler, L. T. Cardoso, A. N. Walker, M. K. Hossain, V. W. Day, E. Nordlander and T. A. Jackson, *Angew Chem Int Ed Engl*, 2017, **56**, 4178-4182; c) A. A. Massie, M. C. Denler, R. Singh, A. Sinha, E. Nordlander and T. A. Jackson, *Chemistry – A European Journal*, 2020, **26**, 900-912.

13. J. G. S. a. H. Saltzman, *Organic syntheses*, 1963, **43**, 65.
14. a) W. K. C. Lo, C. J. McAdam, A. G. Blackman, J. D. Crowley and D. A. McMorran, *Inorganica Chimica Acta*, 2015, **426**, 183-194; b) M. Lubben, A. Meetsma, E. C. Wilkinson, B. Feringa and L. Que Jr, *Angewandte Chemie International Edition in English*, 1995, **34**, 1512-1514; c) M. Mitra, H. Nimir, S. Demeshko, S. S. Bhat, S. O. Malinkin, M. Haukka, J. Lloret-Fillol, G. C. Lisensky, F. Meyer, A. A. Shteinman, W. R. Browne, D. A. Hrovat, M. G. Richmond, M. Costas and E. Nordlander, *Inorganic Chemistry*, 2015, **54**, 7152-7164; d) S. Rana, A. Dey and D. Maiti, *Chemical Communications*, 2015, **51**, 14469-14472.
15. a) R. A. Marcus, *Annual Review of Physical Chemistry*, 1964, **15**, 155-196; b) R. A. Marcus, *Angewandte Chemie International Edition in English*, 1993, **32**, 1111-1121.
16. I. Garcia-Bosch, A. Company, C. W. Cady, S. Styring, W. R. Browne, X. Ribas and M. Costas, *Angewandte Chemie (International ed. in English)*, 2011, **50**, 5648-5653.
17. G. B. Wijeratne, B. Corzine, V. W. Day and T. A. Jackson, *Inorg Chem*, 2014, **53**, 7622-7634.
18. W. J. Song, M. S. Seo, S. DeBeer George, T. Ohta, R. Song, M.-J. Kang, T. Tosha, T. Kitagawa, E. I. Solomon and W. Nam, *Journal of the American Chemical Society*, 2007, **129**, 1268-1277.
19. K. A. Prokop, H. M. Neu, S. P. de Visser and D. P. Goldberg, *Journal of the American Chemical Society*, 2011, **133**, 15874-15877.
20. C. Hansch, A. Leo and R. W. Taft, *Chemical Reviews*, 1991, **91**, 165-195.
21. a) Y. Goto, T. Matsui, S.-i. Ozaki, Y. Watanabe and S. Fukuzumi, *Journal of the American Chemical Society*, 1999, **121**, 9497-9502; b) P. Barman, A. K. Vardhaman, B. Martin, S. J. Wörner, C. V. Sastri and P. Comba, *Angewandte Chemie International Edition*, 2015, **54**, 2095-2099; c) A. K. Vardhaman, P. Barman, S. Kumar, C. V. Sastri, D. Kumar and S. P. de Visser, *Angewandte Chemie International Edition*, 2013, **52**, 12288-12292.
22. J. Chen, K.-B. Cho, Y.-M. Lee, Y. H. Kwon and W. Nam, *Chemical Communications*, 2015, **51**, 13094-13097.
23. J. Jung, S. Kim, Y.-M. Lee, W. Nam and S. Fukuzumi, *Angewandte Chemie International Edition*, 2016, **55**, 7450-7454.
24. Ideally, the $E_{1/2}$ values, rather than E_{ox}, would be used to calculate $-\Delta G_{et}$. Our use of E_{ox} assumes the difference between E_{ox} and $E_{1/2}$ is not large enough to account for the discrepancy between the experimental data and the fitted curve. The basis of this assumption is the low sensitivity of k_{et} on E_{ox}. To illustrate this low sensitivity, Figure S12 shows fits of the data where we assume a reorganization energy of 2.0 eV (taken from the reorganization energy for **1** in outer-sphere electron transfer reactions from Figure 5) and manually and uniformly adjust E_{ox} by -0.25, -0.35, and -0.50 eV. Only when the Marcus curve is adjusted by >350 mV does the curve begin to overlap with some of the data points. These results therefore highlight the low sensitivity of k_{et} to E_{ox}.